Journal of Quantitative Spectroscopy & Radiative Transfer 205 (2018) 184–195

Contents lists available at ScienceDirect

Journal of Quantitative Spectroscopy & Radiative Transfer

journal homepage: www.elsevier.com/locate/jqsrt

A model study of aggregates composed of spherical soot monomers with an acentric carbon shell

Jie Luo, Yongming Zhang, Qixing Zhang*

State Key Laboratory of Fire Science, University of Science and Technology of China, Hefei, Anhui 230026, China

ARTICLE INFO

Article history:
Received 12 May 2017
Revised 26 October 2017
Accepted 28 October 2017
Available online 28 October 2017

Keywords:
Coated soot particles
Acentric core–shell monomers model
Optical properties

ABSTRACT

Influences of morphology on the optical properties of soot particles have gained increasing attentions. However, studies on the effect of the way primary particles are coated on the optical properties is few. Aimed to understand how the primary particles are coated affect the optical properties of soot particles, the coated soot particle was simulated using the acentric core–shell monomers model (ACM), which was generated by randomly moving the cores of concentric core–shell monomers (CCM) model. Single scattering properties of the CCM model with identical fractal parameters were calculated 50 times at first to evaluate the optical diversities of different realizations of fractal aggregates with identical parameters. The results show that optical diversities of different realizations for fractal aggregates with identical parameters cannot be eliminated by averaging over ten random realizations. To preserve the fractal characteristics, 10 realizations of each model were generated based on the identical 10 parent fractal aggregates, and then the results were averaged over each 10 realizations, respectively. The single scattering properties of all models were calculated using the numerically exact multiple-sphere T-matrix (MSTM) method. It is found that the single scattering properties of randomly coated soot particles calculated using the ACM model are extremely close to those using CCM model and homogeneous aggregate (HA) model using Maxwell–Garnett effective medium theory. Our results are different from previous studies. The reason may be that the differences in previous studies were caused by fractal characteristics but not models. Our findings indicate that how the individual primary particles are coated has little effect on the single scattering properties of soot particles with acentric core–shell monomers. This work provides a suggestion for scattering model simplification and model selection.

1. Introduction

Understanding of optical properties of soot particles is extremely important for atmospheric remote sensing, climate change studies and fire detection, etc. However, optical properties of soot particles are still uncertain due to the incomplete understanding of the optical properties of soot aerosols with complex morphologies and chemical compositions [1].

Freshly emitted soot particles generally present fractal structure characteristics, but trend to be coated with non-absorbing aerosols under the influences of the atmospheric aging, which leads to more complex morphologies. Therefore, the research on random non-absorbing coatings is very important for the understanding of scattering properties of soot particles. Soot particles are classified into four categories by China et al. [2]: (1) embedding; (2) partly coating; (3) bare; and (4) internal mixing. This work mainly targets on the partly coated soot particles which is an important component of soot aerosols. The single core–shell (SC) model using the core–mantle Mie theory was commonly applied in climate model to simplify the calculations [3–5]. But the calculation results can lead to large deviation compared with measurements and more realistic models [6–15]. Although many studies have concerned on the optical properties of soot particles with mixing states [7,8,10,16], the effect of the way soot particles are coated on the optical properties is still unclear and few studies investigate how the primary particles are coated influences the optical properties of soot particles.

Soot particles tend to be randomly coated with non-absorbing materials in atmospheric aging. Dong et al. [17] simulated the random coatings by adding dipoles. In that work, whether a discrete dipole is added was dominated by the sum of the inverse square of the distance between the point and every center of monomer sphere. A morphology of coatings submerging the soot monomers can be simulated in this way. However, soot particles may be randomly coated with a thin organic materials layer in some cases. Another alternative model is also commonly applied for calculating

* Corresponding author.
E-mail address: qixing@ustc.edu.cn (Q. Zhang).

https://doi.org/10.1016/j.jqsrt.2017.10.024
0022-4073/

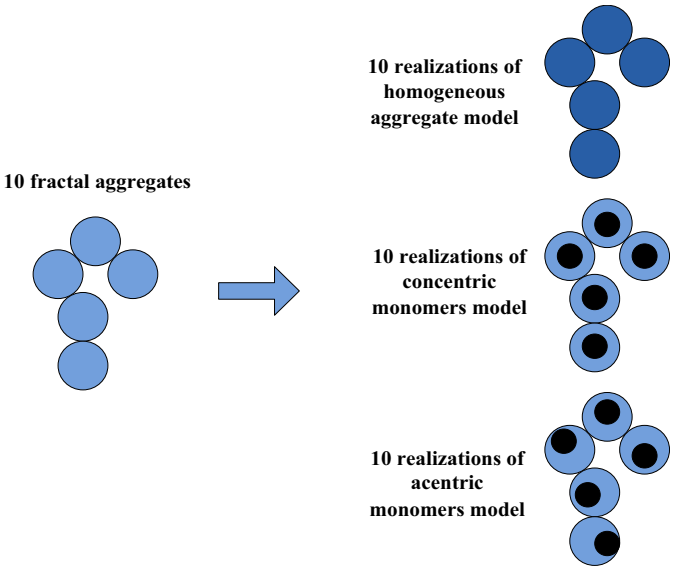

Fig. 1 . The way to preserve fractal nature of different models.

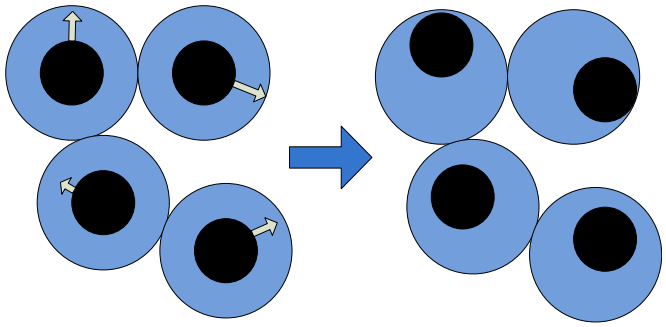

Fig. 2. The generation of acentric core–shell monomers model.

the optical properties of soot particles, which assumes that soot monomers are contacted in point with each other, and every soot monomer is coated by non-absorbing materials with constant thickness. This leads to the intersecting of the coatings and uncertainty of soot volume fractions [18–20]. Wu et al. [18] added dipoles at edges of the whole structure one by one. In that work, a realistic morphology of thinly coated soot particles was simulated. However, the coatings are completely random and not easy to be controlled, so it is hard to understand how primary particles are coated influences the optical properties of soot particles using such model. Another important problem is that the former three models are generally calculated with the discrete dipole approximation (DDA) method [21], and in order to gain accurate calculation results, the dipole number should be considerably large, which leads to relatively higher computational time cost. In order to reduce computation cost, another model was developed, which is composed of concentric core–shell monomers which are contacted in point with each other [20,22,23]. Their optical properties were calculated using the numerically exact multiple-sphere T-matrix (MSTM) method [24,25], which demands for less computational time cost than DDA method [26]. However, the individual primary particles are randomly coated in reality, namely are not the concentric core–shell appearance. Although in reality the soot particles have complex morphology, the model with real shape is very computationally expensive, so it is reasonable to conduct some simplifications. The closed-shell morphology reflect the real morphology to a great extent. It can represents the process of accumulation of a refractory material around individual soot monomers, and is an example of where coating material not only covers the outer layers of soot aggregates but also fills the internal voids among primary spherules. In addition, it is more likely to be put into practice than other models due to the high computation efficiency, so we conduct a detailed study on this morphology. To reflect the randomness of coatings, we proposed the acentric core–shell monomers model, which generated by randomly moving the cores of concentric core–shell monomers model. The aim of this paper is to investigate how the primary particles are coated affects the optical properties. The way primary particles are coated was simulated by changing the movement patterns of soot cores.

The single scattering properties calculated using ACM model were compared with those using SC model, HA model and CCM model. Previous studies [18,23] concluded that the results calculated using HA model, CCM model and more realistic model were different. However, the differences can be also caused by fractal nature but not models. In order to eliminate optical diversities caused by fractal characteristics, the structures of all models were generated based on 10 identical parent fractal aggregates in this study, so all models shared the same structures. In this work, the soot monomer was fixed to be 0.02 um, so the total monomer radius varies with the soot fractions. We generated soot particles with different soot volume fractions by scaling the 10 aggregates generated at first to maintain the fractal characteristics identical.

The generation of models for randomly coated soot particles, the theory and method for calculating the optical properties of the coated soot particle are introduced in Section 2. The random-orientation averaged results of different models are discussed in Section 3. Conclusions are given in Section 4.

2. Models for soot particles coated with random non-absorbing aerosols

In this work, soot particles were simulated using the ACM model. The SC model, HA model, and CCM model were used for comparison. The volumes are same for all models, which is the sums of soot monomers and coatings. The monomer radius of HA model, CCM model and ACM are identical. Differently, the HA model is composed of homogeneous monomers with the single refractive index, while CCM model and ACM model are constructed as two spheres with different refractive indices for the highly absorbing core and the weakly absorbing shell. The difference between the CCM model and the ACM model is that the positions of core centers of acentric core–shell monomers model are random.

2.1. Generations of models for soot particles coated with random non-absorbing aerosols

Diffusion limited aggregation (DLA) algorithm [27] is often applied to generate fractal structures. In this work, the fractal aggregates were generated by a tunable DLA code developed by Wozniak et al. [28]. It preserves fractal parameters at each step of the aggregation compared to the ordinary DLA code. This allows to avoid generation of multi-fractal aggregates [29]. The construction of the fractal structure satisfies the well-known fractal laws [3]:

$$N_s = k_0\left(\frac{R_g}{R}\right)^{D_f} \tag{1}$$

$$R_g{}^2 = \frac{1}{N}\sum_{i=1}^{N_s} l_i{}^2 \tag{2}$$

where N_s is the number of the monomers in the cluster, R is the mean radius of the monomers, k_0 is the fractal prefactor, D_f is the

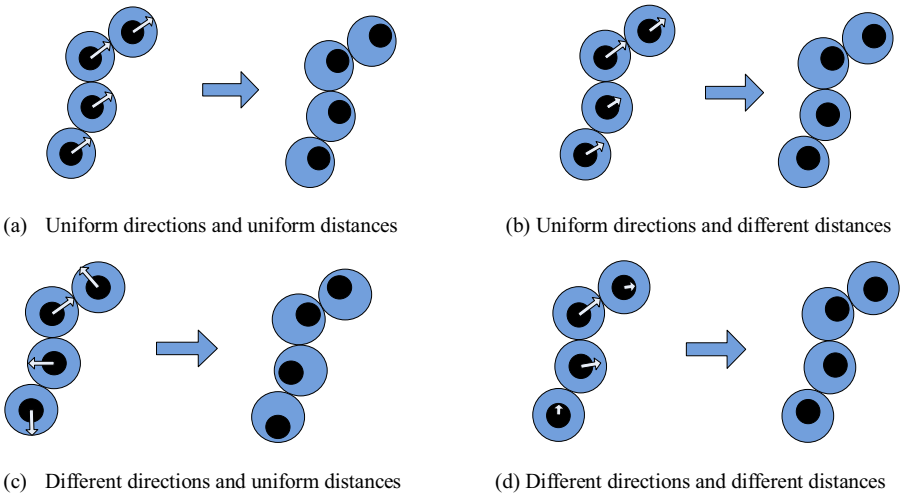

Fig. 3. The method for simulating how the primary particles are coated using different movement patterns.

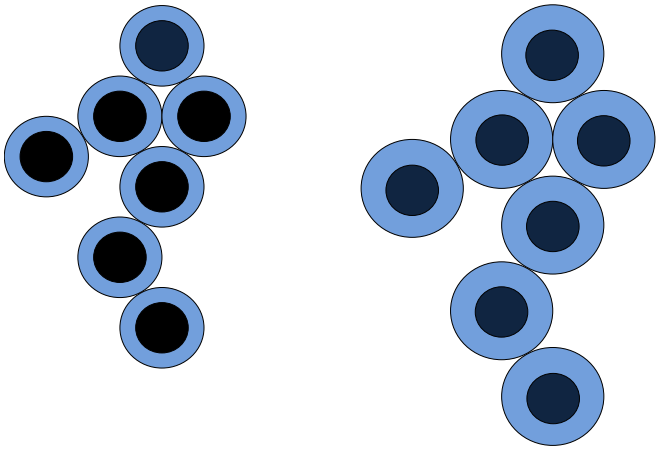

Fig. 4. The way to preserve the fractal nature of concentric monomers model with different soot fractions.

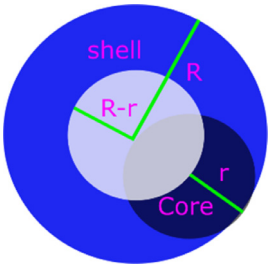

Fig. 5. Region of center of soot core, which is shown as the white area.

Fig. 6. Typical cluster of the soot particles simulated with acentric core–shell monomers model, $N_s = 100$, $D_f = 1.8$, $F_{soot} = 0.4$.

fractal dimension, R_g is the radius of gyration, and l_i is the distance from the ith monomer to the center of the cluster. The fractal prefactor was assumed to be 1.2. The radius of soot monomers was assumed to be a constant even though the optical properties of soot particles is influenced by polydispersity of soot monomers [18,30–32].

To eliminate the optical diversities caused by fractal nature, 10 parent fractal aggregates with identical fractal parameters were generated using tunable DLA algorithm at first, then 10 realizations of different models were all generated based on these 10 fractal aggregates. To be more detail, the 10 realizations of HA model were directly generated using these 10 fractal aggregates. For CCM model, the shells of 10 realizations were generated using these 10 fractal aggregates, then the soot cores which share the identical centers as shells were added. The generation of ACM model was similar to the CCM model, but the soot cores of acentric core–shell model are random. Then the results of each model were averaged over the 10 realizations. The way to preserve fractal nature for different models is shown in Fig. 1. In addition, the soot monomer radius is fixed to be 0.02 um, and different soot fractions translate to different amount of coating materials, so the radius of monomers varies with different volume fractions. To make the fractal characteristics identical, we generated soot particles with different soot volume fractions by scaling the 10 parent aggregate at first, and then the soot cores were added. The fractal characteristics are preserved, because the fractal law is still satisfied when scaling the whole structure. Fig. 4 shows the way to preserve the fractal nature of concentric monomers model with different soot fractions using concentric monomers model. In order to guarantee the cores non-intersecting with shells, for each monomer, the center of core is randomly located in the sphere which share the identical center with shell and the radius equal to the radius of shell minus the radius of core, as shown in Fig. 5. The generation of ACM model is displayed in Fig. 2. The method for simulating how the way the primary particles are coated using different movement patterns is shown in Fig. 3. The uniform distance was fixed to be

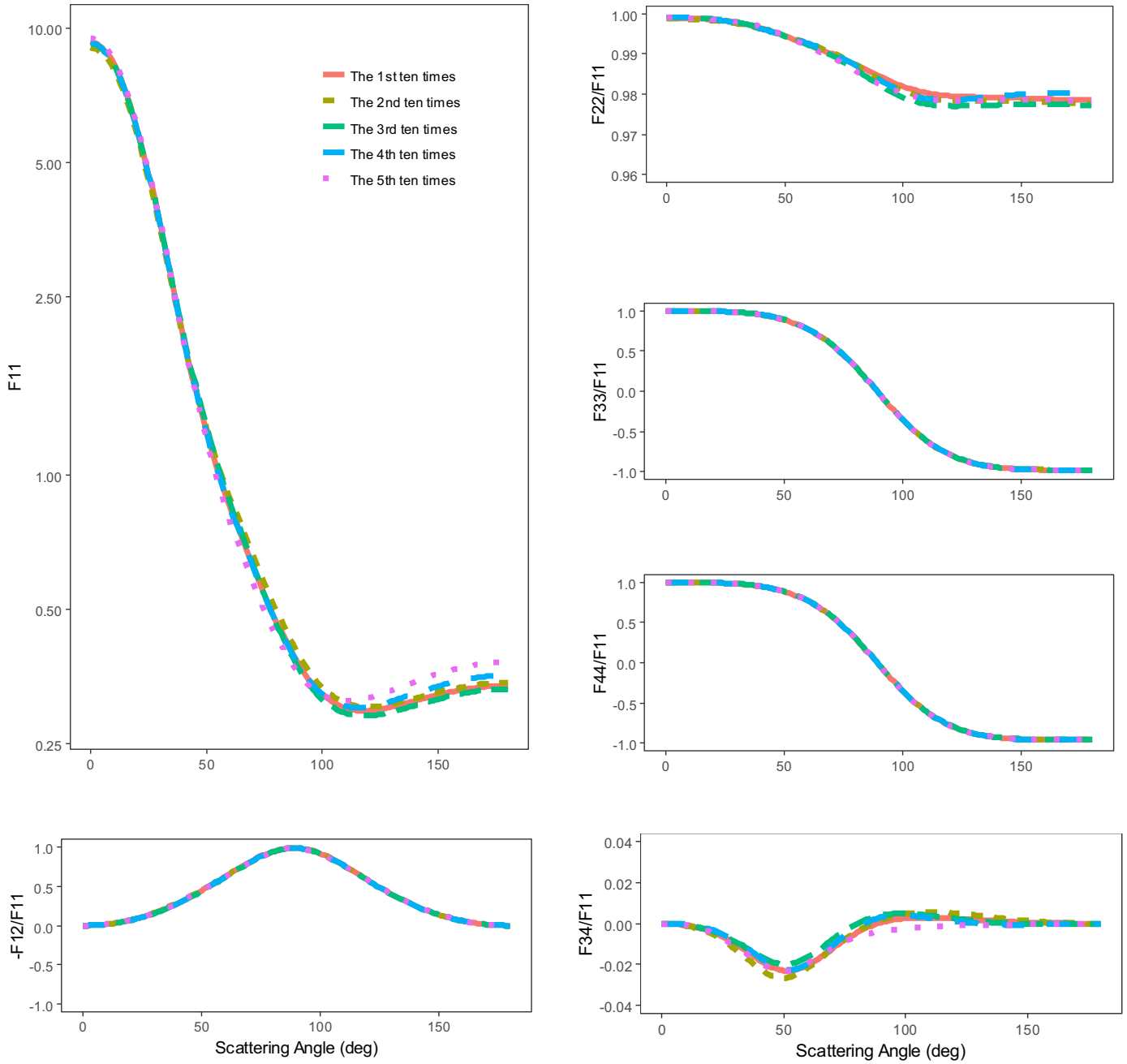

Fig. 7. 50 calculation results of scattering matrices with concentric core–shell monomers model, which are randomly averaged for each 10 calculations, $N_s = 100$, $D_f = 1.8$, $r = 0.02$ um, $\lambda = 0.55$ um, $F_{soot} = 0.6$.

$0.95(R_{shell} - R_{core})$ in this work. Fig. 6 shows typical clusters of the soot particles simulated with ACM model. The monomer number (N_s) is 100, the volume fraction of soot (F_{soot}) is 0.4 and the fractal dimension is 1.8 for example.

For HA model, CCM model and ACM model, the radius of monomers satisfies Eqs. (3)–(5) [23]:

$$V_{soot} = F_{soot} V_{total} \tag{3}$$

$$\frac{4}{3}\pi r^3 = F_{soot}\frac{4}{3}\pi R^3 \tag{4}$$

$$R = \frac{r}{\sqrt[3]{F_{soot}}} \tag{5}$$

where R is the radius of total monomer, r is the radius of soot monomer, F_{soot} is the volume fractions of soot monomer, V_{soot} and V_{total} are volumes of soot monomers and total monomers respectively. According to the SEM and TEM images, soot aggregates are composed of numbers of soot monomers with radius of 0.01–0.03 um [33]. The radius of soot cores was fixed to be 0.02 um in this work, and different soot fractions translate to different amount of coating material. For the SC model, the radius of core and shell (R_{core} and R_{shell}) can be obtained using Eqs. (6) and (7) [18]:

$$R_{core} = \sqrt[3]{N_s} r \tag{6}$$

$$R_{shell} = \sqrt[3]{\frac{N_s}{F_{soot}}} r \tag{7}$$

where N_s is the number of the monomers in the cluster, r is the radius of soot cores, F_{soot} is the volume fractions of soot monomers.

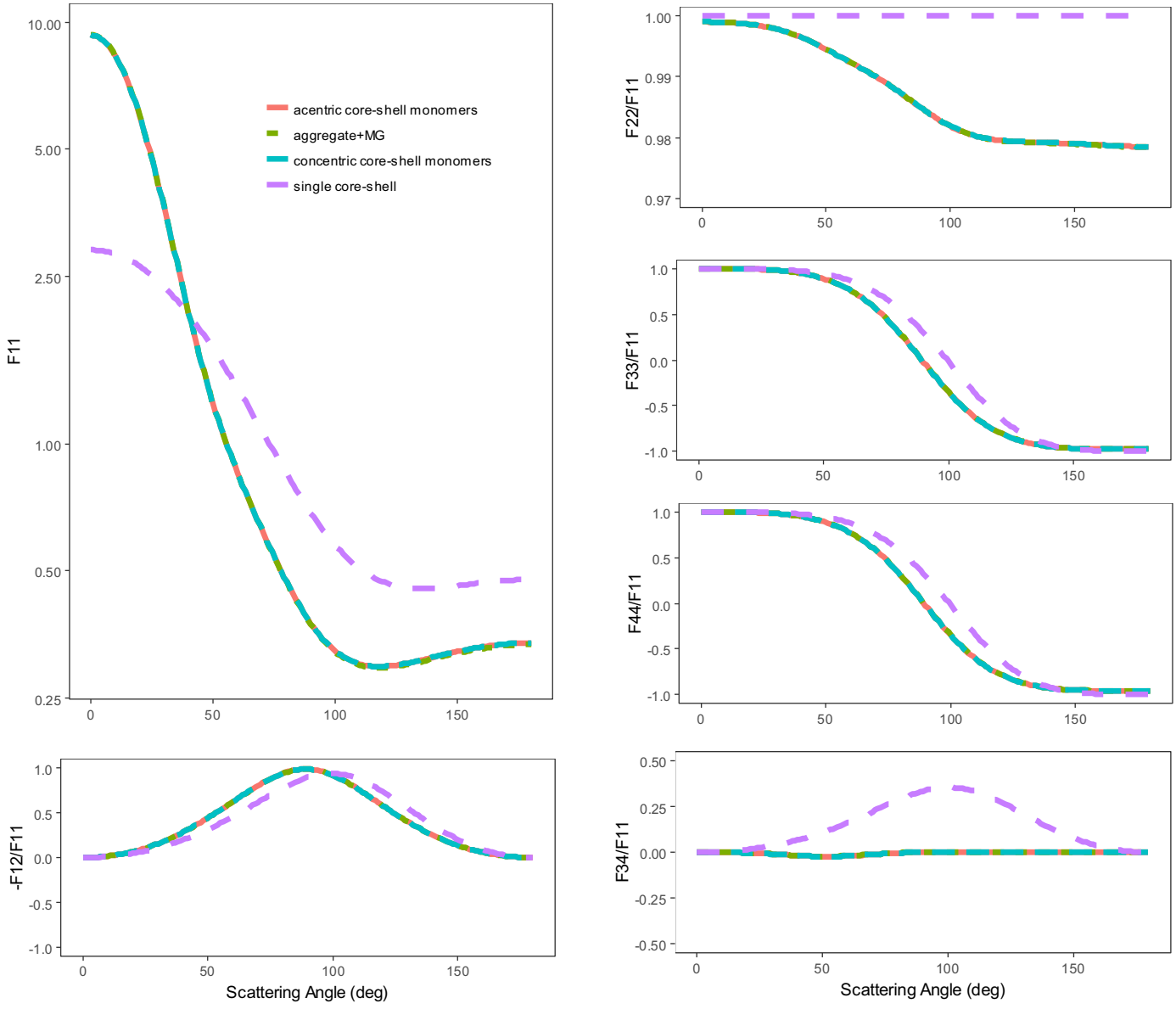

Fig. 8. Scattering matrices of coated soot particles calculated using different models, $N_s = 100$, $D_f = 1.8$, $r = 0.02$ um, $\lambda = 0.55$ um, $F_{soot} = 0.6$.

Table 1
The integrally optical characteristics of coated soot particles calculated using different models with different soot volume fractions ($F_{soot} = 0.2, 0.4, 0.6, 0.8, 1.0$), $N_s = 100$, $D_f = 1.8$, $r = 0.02$ um, $\lambda = 0.55$ um.

Model	Fsoot	Cabs	Csca	SSA	ASY
Acentric core–shell monomers	0.2	0.047227	0.036810	0.645713	0.438021
	0.4	0.042919	0.016927	0.594284	0.282843
	0.6	0.040464	0.011837	0.558734	0.226325
	0.8	0.038714	0.009629	0.534288	0.199181
	1	0.037300	0.008380	0.514860	0.183450
Concentric core–shell monomers	0.2	0.047755	0.036812	0.645181	0.435300
	0.4	0.043171	0.016933	0.594152	0.281721
	0.6	0.040549	0.011840	0.558723	0.225996
	0.8	0.038714	0.009628	0.534288	0.199160
	1	0.037300	0.008380	0.514860	0.183450
Aggregate + MG	0.2	0.046669	0.036690	0.647725	0.440141
	0.4	0.042888	0.016863	0.596575	0.282228
	0.6	0.040485	0.011786	0.560525	0.225481
	0.8	0.038775	0.009610	0.535255	0.198612
	1	0.037300	0.008380	0.514860	0.183450
Single core–shell	0.2	0.072598	0.092727	0.596630	0.560876
	0.4	0.057447	0.047221	0.435560	0.451149
	0.6	0.050067	0.035362	0.343430	0.413932
	0.8	0.045522	0.028823	0.298090	0.387698
	1	0.042155	0.024408	0.272080	0.366693

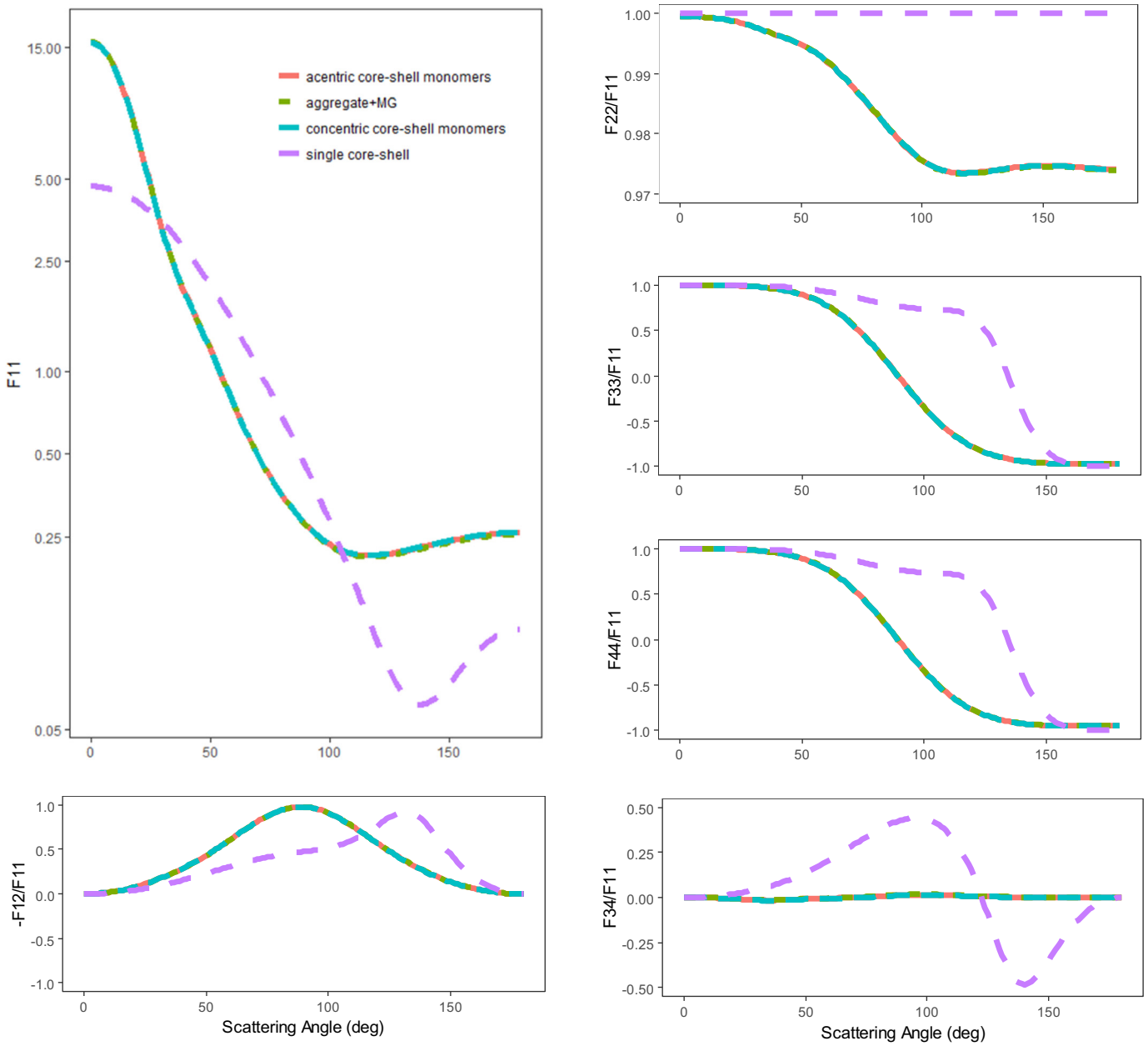

Fig. 9. Scattering matrices of coated soot particles calculated using different models, $N_s = 100$, $D_f = 1.8$, $r = 0.02$ um, $\lambda = 0.55$ um, $F_{soot} = 0.2$.

The optical properties of soot particles were investigated for a visible wavelength at 0.55 um, and the refractive index was assumed to be $1.95 + 0.79i$ [18,34]. The coatings were assumed to be organic carbon with a refractive index of constant 1.55 according to Chakrabarty et al. [35]. The refractive indices of the homogeneous aggregate model were obtained using Maxwell–Garnett (MG) effective medium theory [36], which is a sound approach provided that the size parameter of the inclusions is smaller than a threshold value [37–40]. In this work, the MG effective medium is applied to primary particles, whose size parameter is small.

2.2. Theory and method

Recently, the MSTM method has been developed to calculate the arbitrary configurations of spheres without overlapping [25,41–44]. Different from other numerical methods, the MSTM method calculates the optical properties of randomly oriented particles analytically without numerical averaging over particle orientations, so the efficiency is higher than most other numerical methods such as discrete dipole approximation (DDA) method [21,26]. The MSTM Version 3.0 [45] which updated in 2013 was applied for all models in this study.

Due to the random distribution of soot particles, the normalized stokes scattering matrix has the well-known structure with six independent elements which related to the scattering angle [46]:

$$\begin{bmatrix} F_{11}(\theta) & F_{12}(\theta) & 0 & 0 \\ F_{12}(\theta) & F_{22}(\theta) & 0 & 0 \\ 0 & 0 & F_{33}(\theta) & F_{34}(\theta) \\ 0 & 0 & -F_{34}(\theta) & F_{44}(\theta) \end{bmatrix} \tag{8}$$

The element $F_{11}(\theta)$ is well-known as phase function, which satisfies the normalization formulation:

$$\frac{1}{2}\int_0^{\pi} F_{11}(\theta) sin\theta d\theta = 1 \tag{9}$$

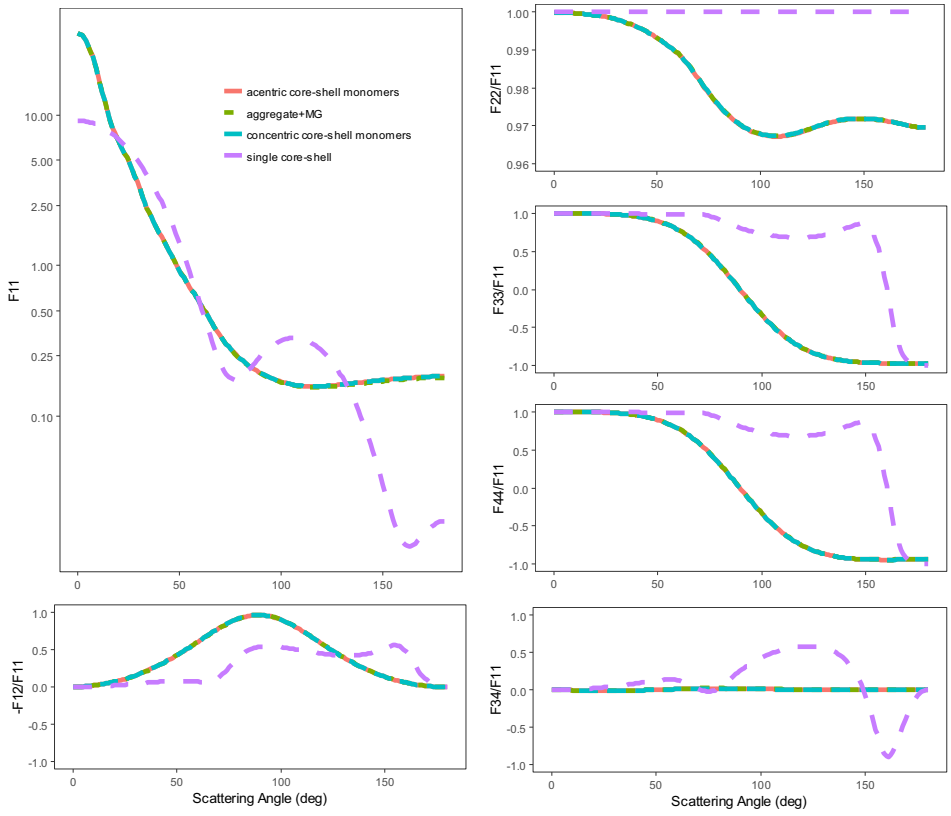

Fig. 10. Scattering matrices of coated soot particles calculated using different models, $N_s = 300$, $D_f = 1.8$, $r = 0.02$ um, $\lambda = 0.55$ um, $F_{soot} = 0.2$.

Moreover, the element $-F_{12}(\theta)/F_{11}(\theta)$ indicates the variation of the polarization of scattered light, the $F_{22}(\theta)/F_{11}(\theta)$ can be used to evaluate the total nonsphericity for the whole cluster. Scattering parameters concerning integral characteristics such as the optical cross sections, the single scattering albedo and the asymmetry parameter were also calculated in this study.

For HA model, the effective refractive index was gained by using MG effective medium theory [3]:

$$\frac{\varepsilon_{eff} - \varepsilon_2}{\varepsilon_{eff} + 2\varepsilon_2} = F_{soot}\frac{\varepsilon_1 - \varepsilon_2}{\varepsilon_1 + 2\varepsilon_2} \tag{10}$$

$$m_{eff} = \sqrt{\varepsilon_{eff}} \tag{11}$$

where F_{soot} is the volume fraction of soot monomers, ε_1 is the permittivity of soot monomers, ε_2 is the permittivity of non-absorbing coatings, ε_{eff} and m_{eff} are effective permittivity and effective refractive index respectively.

3. Results and discussion

The fractal structures of soot particles may be diverse even though the fractal parameters are identical. Many studies averaged over five or ten realizations to reflect their general optical properties [17,18,26]. But the optical diversities caused by fractal characteristics may be not fully eliminated with this method, so it can introduce errors for model comparison. In order to evaluate whether the optical diversities of different realizations of fractal aggregates can be eliminated by averaging over ten calculations, the scattering matrices of soot particles were calculated 50 times using CCM model with the same fractal parameters. Results were randomly classified into 5 groups, and then 10 calculation results were averaged in each group. Fig. 7 indicates that optical diversities of different realizations of fractal aggregates with identical parameters cannot be completely eliminated by averaging over 10 realizations. Furthermore, the tunable DLA code applied in this work avoided generation of multi-fractal aggregates, so lager optical diversities may be brought when adopting the ordinary DLA code. In order to preserve fractal nature, 10 parent fractal aggregates with identical parameters were generated at first. Then 10 realizations of different models were all generated based on these 10 fractal aggregates, so that all the models shared the identical fractal structures. This handling method for different models is different from previous studies [17,18,26], which randomly generated new aggregates for each model.

Fig. 8 compares the scattering matrices calculated using different models for the exactly identical fractal parameters in study [18]. All the elements of scattering matrices calculated using the ACM model are significantly different from those using SC model. Therefore, the scattering properties of soot particles cannot be calculated using the widely used SC model. However, all the elements of scattering matrices calculated using the ACM model are extremely close to those with CCM and HA (aggregate + MG) model, which is different from previous studies [18,23], where the scattering matrices calculated using CCM model and HA model were different. The reason may be that the optical diversities in previous studies were induced by fractal characteristics but not the models.

To investigate how the number of primary particles and soot volume fractions influences the optical diversities for different models, the comparison of independent elements of normalized stokes scattering matrices for different models with $F_{soot} = 0.2$, $D_f = 1.8$ are shown in Figs. 9 and 10 and the numbers of primary particles are 100 and 300 respectively. In these cases, the soot particles present a chain-like fractal structure, and the soot volume fraction should be greater than 0.4, because those soot particles with thicker coatings tend to be nearly spherical particles [18,47].

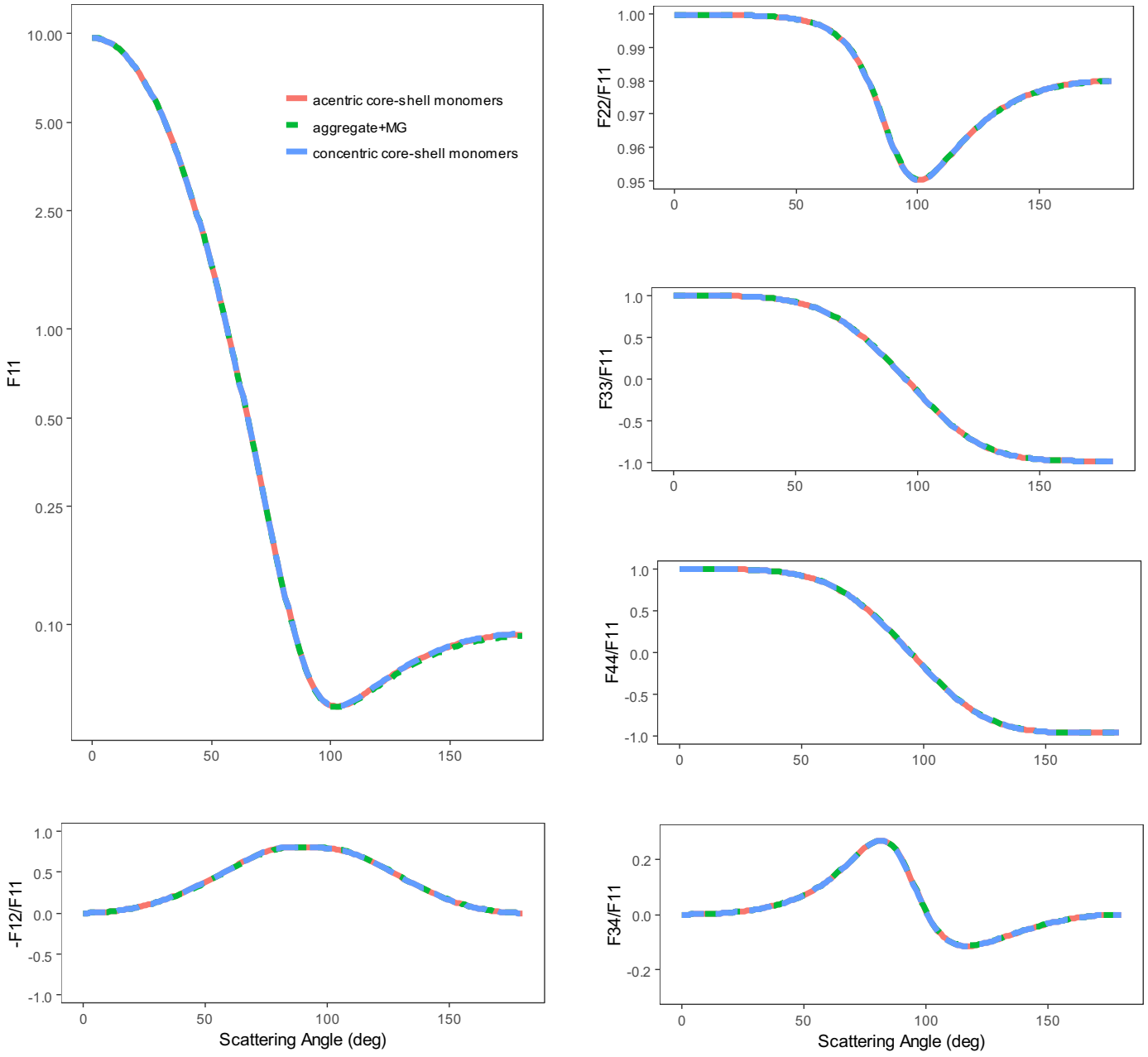

Fig. 11. Scattering matrices of coated soot particles calculated using different models, $N_s = 100$, $D_f = 2.5$, $r = 0.02$ um, $\lambda = 0.55$ um, $F_{soot} = 0.2$.

However, it is assumed that $F_{soot} \geq 0.2$ to amplify the influences of random coatings. It can be seen from Figs. 8 and 9 that all the elements of scattering matrices calculated using the ACM model are extremely close to those using CCM model and HA model even the soot volume fraction $F_{soot} = 0.2$. It can be easily understood that scattering matrices calculated with the three models are also close when $F_{soot} \geq 0.2$.

In order to investigate whether the optical diversities of different models are influenced by the compact degree of soot particles morphology, the scattering matrices of soot particles with a more compact morphology where $D_f = 2.5$ were calculated using different models. As shown in Fig. 11, scattering matrices calculated using the ACM model, CCM model, and HA model are also extremely close when $D_f = 2.5$. It can be inferred that the compact degree of soot particles has little effect on the optical diversities of the three models.

For better understanding of how the way the primary particles are coated influencing the optical properties of soot particles, the way primary particles are coated was simulated by changing the movement patterns of soot cores. The scattering matrices calculated using ACM model with different movement patterns are shown in Fig. 12. It shows that the optical properties calculated using ACM model with different movement patterns are also extremely close. Combined of Figs. 8–12, it can be concluded that the way how the individual primary particles are coated has negligible influences on the single scattering properties of soot particles.

The Fig. 13 is used for evaluating how the single scattering properties depend on the soot volume fractions. Because the soot monomer radius is fixed to be 0.02 um, so smaller soot fractions translate to thicker coating materials. As shown in Fig. 13, thicker non-absorbing coatings can strengthen forward scattering but weaken backward scattering. Besides, the nonsphericity of soot

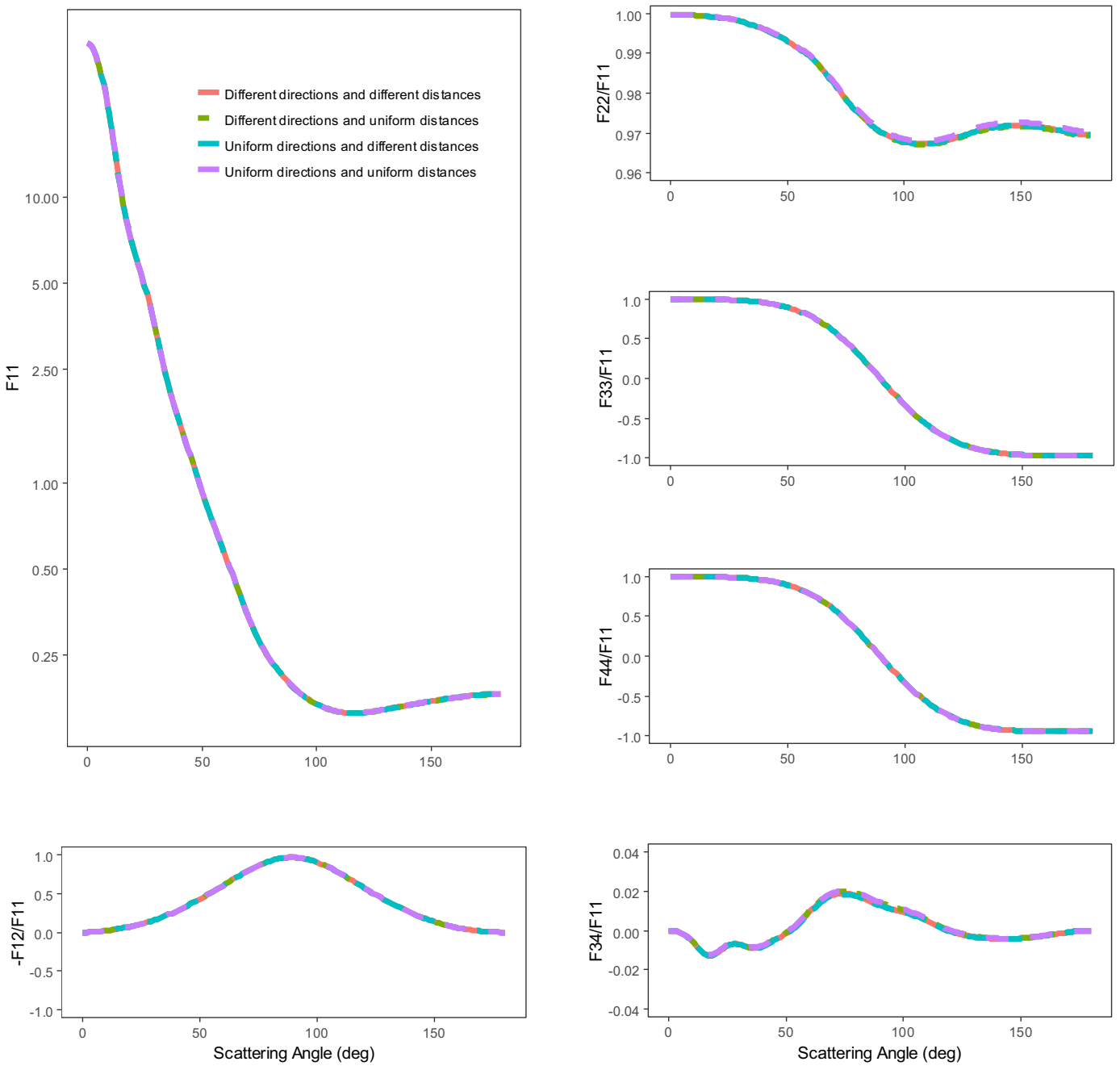

Fig. 12. Scattering matrices of coated soot particles calculated using acentric core–shell monomers model with different movement patterns of soot cores, $N_s = 300$, $D_f = 1.8$, $r = 0.02$ um, $\lambda = 0.55$ um, $F_{soot} = 0.2$.

particles is also strengthened with the decreases of soot volume fractions. In addition, the curves of $F_{34}(\theta)/F_{11}(\theta)$ are from convex to concave, and the minimum point moves forward with the decrease of soot volume fraction. Furthermore, the values of $F_{34}(\theta)/F_{11}(\theta)$ become larger when the coatings get thicker.

The sensitivities of scattering matrices to soot monomers number are shown in Fig. 14. It indicates that the forward scattering is enhanced by the increase of soot monomer numbers, but the backward scattering is weakened. Moreover, a more remarkable nonsphericity can be brought by increasing the soot monomers number and the salient points of curves of $F_{34}(\theta)/F_{11}(\theta)$ move forward when the soot monomer numbers increased.

The absorption across sections (Cabs), scattering cross sections (Csca), single scattering albedo (SSA) and asymmetry parameter (ASY) of coated soot particles with different soot volume fractions ($F_{soot} = 0.2,\ 0.4,\ 0.6,\ 0.8,\ 1.0$) were calculated using different models. As shown in Table 1, the integrally optical characteristics of SC model are obviously different from the other three models. The SC model overestimates the absorption/scattering cross sections and single scattering albedo but underestimates the asymmetry parameter. Therefore, these optical effects caused by the model simplification is necessary to be considered. Besides, thicker coatings can lead to larger differences between SC model and the other three models in absorption/scattering cross sections, but smaller differences in single scattering albedo and asymmetry.

Nevertheless, the integrally optical characteristics of ACM model, CCM model and HA model are extremely close. For these three models, the errors of all elements are within 3%, which

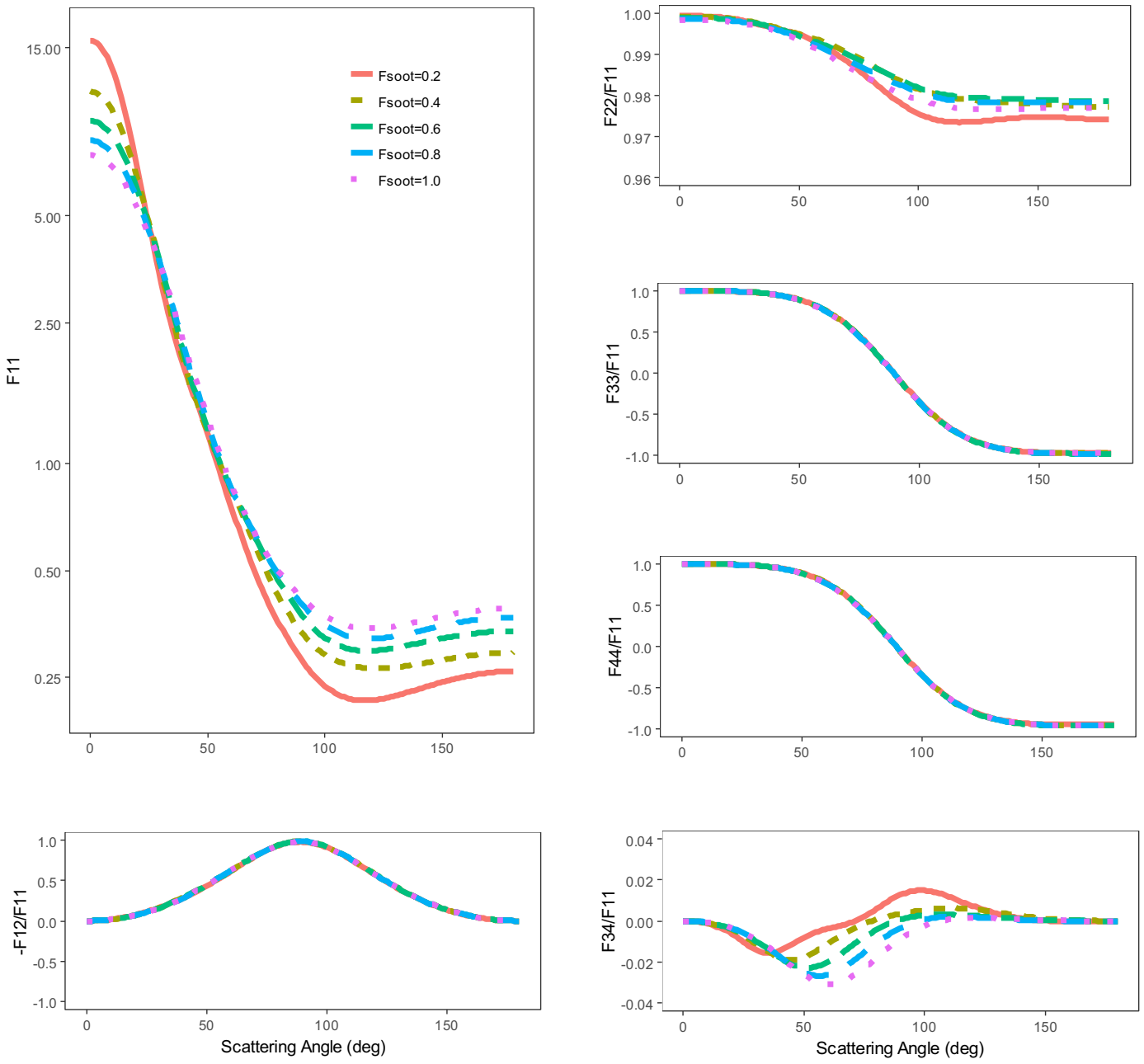

Fig. 13. Scattering matrices of coated soot particles with different soot volume fractions (F_{soot} = 0.2, 0.4, 0.6, 0.8, 1.0), N_s = 100, D_f = 1.8, r = 0.02 um, λ = 0.55 um.

verifies that the randomness of coatings has negligible influence on soot particles with acentric core–shell spherical monomers. It can be observed from Table 1 that the absorption/scattering cross sections and single scattering albedo of randomly coated soot particles are enlarged with the decrease of soot volume fraction, which is consistent with other studies [11,12,17]. This shows that the random coatings can amplify the absorption/scattering cross sections. Moreover, the amplification of scattering cross section is larger than absorption cross section.

4. Summary and conclusions

For a better understanding of how the way primary particles are coated influencing the optical properties of soot particles, a comparative model study has been conducted. The soot particles were simulated using ACM model, while the SC model, HA model and CCM model were selected for comparison. The ACM model was generated by randomly moving the soot cores of CCM model.

The results show that the single scattering properties calculated using the ACM model are extremely close to those using CCM model and HA model. This is different from results in other studies where the scattering matrices were different by using CCM model and HA model. The reason may be that the differences in previous study were caused by fractal characteristics. In order to preserve fractal characteristics, the fractal structures of all models were generated based on the identical parent 10 aggregates. Because the soot core is fixed to be 0.02 um, so different soot fractions translate to different amount of coating material. Therefore, the monomers radius may be diverse when soot fractions is different. The whole structure of soot particles with different soot volume fractions was scaled to maintain the fractal characteristics identical. Then the single scattering results are averaged by

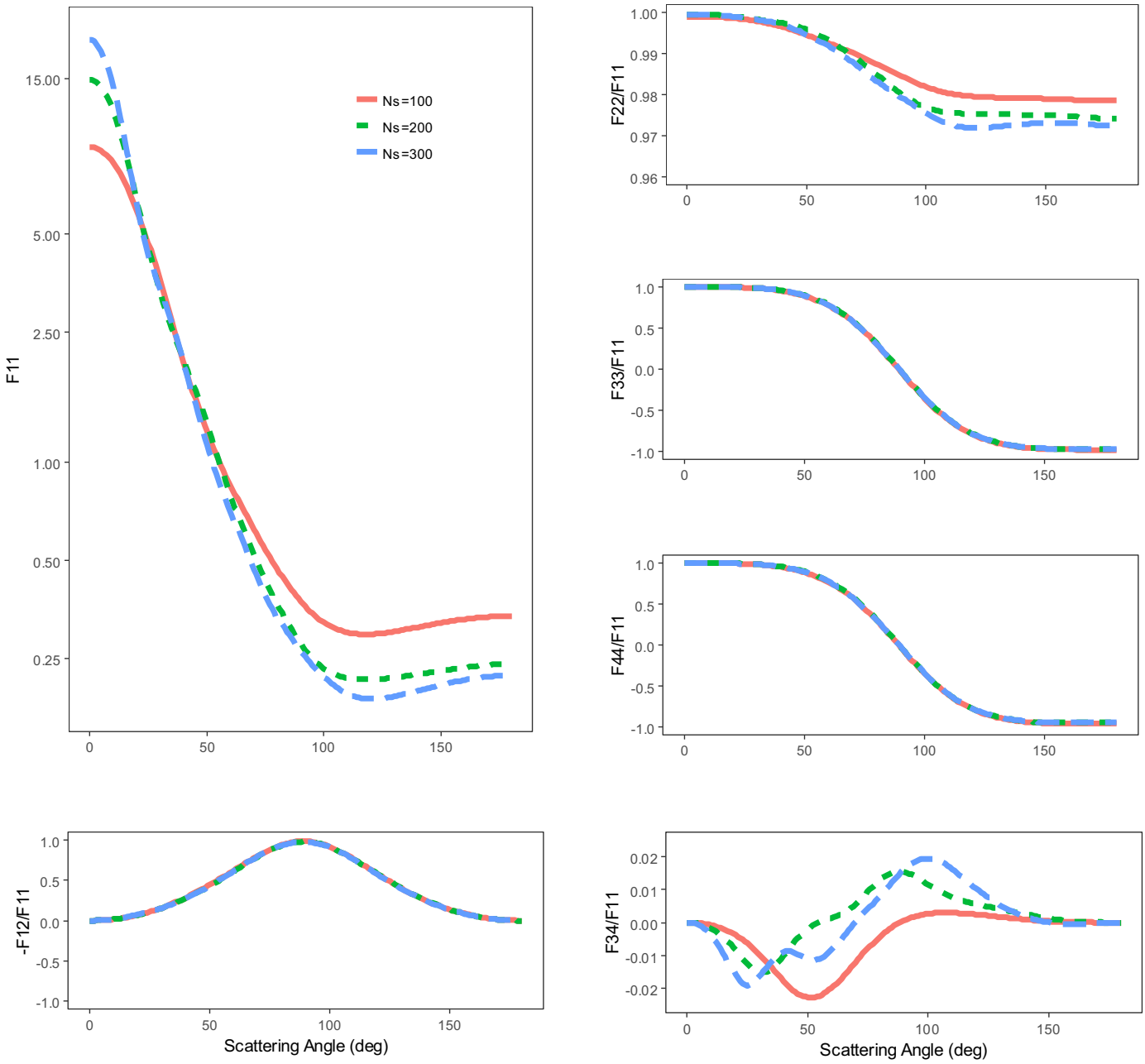

Fig. 14. Scattering matrices of coated soot particles with different soot monomer numbers ($N_s = 100, 200, 300$), $D_f = 1.8$, $r = 0.02$ um, $\lambda = 0.55$ um, $F_{soot} = 0.6$.

10 realizations where all models shared identical fractal structures. For better understanding of the influences of non-absorbing coatings, the way primary particles are coated were simulated using different movement patterns. It can be concluded that the way how the primary particles are coated has negligible effects on the single scattering properties of soot particles. Therefore, soot particles with acentric core–shell monomers can be modeled with CCM model and HA model for simplifying calculations when using MSTM method.

The results also demonstrate that the SC model can lead large errors in scattering matrices. In addition, the optical properties are significantly influenced by soot volume fractions. The decreases of soot volume fractions can strengthen forward scattering, but weaken backward scattering. Furthermore, the absorption/scattering cross sections turns larger when the coatings become thicker.

Acknowledgments

We particularly thank Dr. D. W. Mackowski and Dr. M. I. Mishchenko for the MSTM code. This work was financially supported by the National Natural Science Foundation of China under grant no. 41675024, National Key Research and Development Plan under grant no. 2016YFC0800100, and Anhui Provincial Key Research and Development Program under grant no. 1704a0902030. The authors gratefully acknowledge all of these supports.

References

[1] Cappa CD, Onasch TB, Massoli P, Worsnop DR, Bates TS, Cross ES, et al. Radiative absorption enhancements due to the mixing state of atmospheric black carbon. Science 2012;337:1078–81.
[2] China S, Mazzoleni C, Gorkowski K, Aiken AC, Dubey MK. Morphology and mixing state of individual freshly emitted wildfire carbonaceous particles. Nat Commun 2013;4:2122.

[3] Mishchenko MI, Travis LD, Lacis AA. Scattering, absorption, and emission of light by small particles. Cambridge; New York: Cambridge University Press; 2002.
[4] Lack DA, Cappa CD. Impact of brown and clear carbon on light absorption enhancement, single scatter albedo and absorption wavelength dependence of black carbon. Atmos Chem Phys 2010;10:4207–20.
[5] Liu DT, Whitehead J, Alfarra MR, Reyes-Villegas E, Spracklen DV, Reddington CL, et al. Black-carbon absorption enhancement in the atmosphere determined by particle mixing state. Nat Geosci 2017;10 184-U32.
[6] Liu L, Mishchenko MI, Patrick Arnott W. A study of radiative properties of fractal soot aggregates using the superposition T-matrix method. J Quant Spectrosc Radiat Transf 2008;109:2656–63.
[7] Kahnert M, Nousiainen T, Lindqvist H, Ebert M. Optical properties of light absorbing carbon aggregates mixed with sulfate assessment of different model geometries for climate forcing calculations. Opt Express 2012;20:10042–58.
[8] Kahnert M, Nousiainen T, Lindqvist H. Models for integrated and differential scattering optical properties of encapsulated light absorbing carbon aggregates. Opt Express 2013;21:7974–93.
[9] Yon J, Liu F, Bescond A, Caumont-Prim C, Rozé C, Ouf F-X, et al. Effects of multiple scattering on radiative properties of soot fractal aggregates. J Quant Spectrosc Radiat Transf 2014;133:374–81.
[10] Wu Y, Cheng T, Zheng L, Chen H, Xu H. Single scattering properties of semi-embedded soot morphologies with intersecting and non-intersecting surfaces of absorbing spheres and non-absorbing host. J Quant Spectrosc Radiat Transf 2015;157:1–13.
[11] Cheng T, Wu Y, Gu X, Chen H. Effects of mixing states on the multiple-scattering properties of soot aerosols. Opt Express 2015;23:10808–21.
[12] Doner N, Liu FS, Yon J. Impact of necking and overlapping on radiative properties of coated soot aggregates. Aerosol Sci Technol 2017;51:532–42.
[13] Yon J, Bescond A, Liu F. On the radiative properties of soot aggregates part 1: necking and overlapping. J Quant Spectrosc Radiat 2015;162:197–206.
[14] Liu FS, Yon J, Bescond A. On the radiative properties of soot aggregates—part 2: effects of coating. J Quant Spectrosc Radiat 2016;172:134–45.
[15] Mackowski DW. A simplified model to predict the effects of aggregation on the absorption properties of soot particles. J Quant Spectrosc Radiat 2006;100:237–49.
[16] Kahnert M, Nousiainen T, Lindqvist H, Ebert M. Optical properties of light absorbing carbon aggregates mixed with sulfate: assessment of different model geometries for climate forcing calculations. Opt Express 2012;20.
[17] Dong J, Zhao JM, Liu LH. Morphological effects on the radiative properties of soot aerosols in different internally mixing states with sulfate. J Quant Spectrosc Radiat Transf 2015;165:43–55.
[18] Wu Y, Cheng T, Zheng L, Chen H. Models for the optical simulations of fractal aggregated soot particles thinly coated with non-absorbing aerosols. J Quant Spectrosc Radiat Transf 2016;182:1–11.
[19] Khalizov AF, Xue H, Wang L, Zheng J, Zhang R. Enhanced light absorption and scattering by carbon soot aerosol internally mixed with sulfuric acid. J Phys Chem A 2009;113:1066–74.
[20] Soewono A, Rogak SN. Morphology and optical properties of numerically simulated soot aggregates. Aerosol Sci Technol 2013;47:267–74.
[21] Draine BT, Flatau PJ. Discrete-dipole approximation for scattering calculations. JOSA A 1994;11:1491–9.
[22] Adler G, Riziq AA, Erlick C, Rudich Y. Effect of intrinsic organic carbon on the optical properties of fresh diesel soot. Proc Natl Acad Sci USA 2010;107:6699–704.
[23] Wu Y, Cheng T, Gu X, Zheng L, Chen H, Xu H. The single scattering properties of soot aggregates with concentric core–shell spherical monomers. J Quant Spectrosc Radiat Transf 2014;135:9–19.
[24] Mishchenko MI, Liu L, Travis LD, Lacis AA. Scattering and radiative properties of semi-external versus external mixtures of different aerosol types. J Quant Spectrosc Radiat Transf 2004;88:139–47.
[25] Mackowski DW, Mishchenko MI. A multiple sphere T-matrix Fortran code for use on parallel computer clusters. J Quant Spectrosc Radiat Transf 2011;112:2182–92.
[26] Liu C, Li J, Yin Y, Zhu B, Feng Q. Optical properties of black carbon aggregates with non-absorptive coating. J Quant Spectrosc Radiat Transf 2017;187:443–52.
[27] Hentschel HGE. Fractal dimension of generalized diffusion-limited aggregates. Phys Rev Lett 1984;52:212–15.
[28] Wozniak M, Onofri FRA, Barbosa S, Yon J, Mroczka J. Comparison of methods to derive morphological parameters of multi-fractal samples of particle aggregates from TEM images. J Aerosol Sci 2012;47:12–26.
[29] Hanan WG, Heffernan DM. Multifractal analysis of the branch structure of diffusion-limited aggregates. Phys Rev E 2012;85 021407-1-10.
[30] Wu Y, Cheng T, Zheng L, Chen H. A study of optical properties of soot aggregates composed of poly-disperse monomers using the superposition T-matrix method. Aerosol Sci Technol 2015;49:941–9.
[31] Charalampopoulos TT, Shu G. Effects of polydispersity of chain-like aggregates on light-scattering properties and data inversion. Appl Opt 2002;41:723–33.
[32] Yin JY, Liu LH. Influence of complex component and particle polydispersity on radiative properties of soot aggregate in atmosphere. J Quant Spectrosc Radiat Transf 2010;111:2115–26.
[33] Aggarwal S, Motevalli V. Investigation of an approach to fuel identification for non-flaming sources using light-scattering and ionization smoke detector response. Fire Saf J 1997;29:99–112.
[34] Bond TC, Bergstrom RW. Light absorption by carbonaceous particles: an investigative review. Aerosol Sci Technol 2006;40:27–67.
[35] Chakrabarty RK, Moosmüller H, Chen LWA, Lewis K, Arnott WP, Mazzoleni C, et al. Brown carbon in tar balls from smoldering biomass combustion. Atmos Chem Phys 2010;10:6363–70.
[36] Garnett JCM. Colours in metal glasses, in metallic films, and in metallic solutions. T R Soc Lond 1906;205:237–88.
[37] Mishchenko MI, Dlugach ZM, Zakharova NT. Direct demonstration of the concept of unrestricted effective-medium approximation. Opt Lett 2014;39:3935–8.
[38] Liu C, Panetta RL, Yang P. Inhomogeneity structure and the applicability of effective medium approximations in calculating light scattering by inhomogeneous particles. J Quant Spectrosc Radiat 2014;146:331–48.
[39] Mishchenko MI, Dlugach JM, Liu L. Applicability of the effective-medium approximation to heterogeneous aerosol particles. J Quant Spectrosc Radiat 2016;178:284–94.
[40] Mishchenko MI, Dlugach JM, Yurkin MA, Bi L, Cairns B, Liu L, et al. First-principles modeling of electromagnetic scattering by discrete and discretely heterogeneous random media. Phys Rep 2016;632:1–75.
[41] Mackowski DW, Mishchenko MI. Calculation of the T matrix and the scattering matrix for ensembles of spheres. J Opt Soc Am A 1996;13:2266–78.
[42] Mackowski DW. A general superposition solution for electromagnetic scattering by multiple spherical domains of optically active media. J Quant Spectrosc Radiat Transf 2014;133:264–70.
[43] Mackowski DW. Calculation of total cross-sections of multiple-sphere clusters. J Opt Soc Am A 1994;11:2851–61.
[44] Mackowski DW, Mishchenko MI. Calculation of the T matrix and the scattering matrix for ensembles of spheres. J Opt Soc Am A 1996;13:2266–78.
[45] http://www.eng.auburn.edu/~dmckwski/scatcodes/.
[46] Chakrabarty RK, Moosmüller H, Arnott WP, Garro MA, Slowik JG, Cross ES, et al. Light scattering and absorption by fractal-like carbonaceous chain aggregates. Comparison of theories and experiment. Appl Opt 2007;46:6990–7006.
[47] Zhang R, Khalizov AF, Pagels J, Zhang D, Xue H, McMurry PH. Variability in morphology, hygroscopicity, and optical properties of soot aerosols during atmospheric processing. Proc Natl Acad Sci USA 2008;105:10291–6.